• Clinical Research •

Different damage patterns of retinal nerve fiber layer and ganglion cell-inner plexiform layer between early glaucoma and non-glaucomatous optic neuropathy

Hui Xiao, Xing Liu, Ping Lian, Ling–Ling Liao, Yi–Min Zhong

State Key Laboratory of Ophthalmology, Zhongshan Ophthalmic Center, Sun Yat-sen University, Guangzhou 510060, Guangdong Province, China

Correspondence to: Xing Liu. State Key Laboratory of Ophthalmology, Zhongshan Ophthalmic Center, Sun Yat-sen University, Jinshui Road No.7, Tianhe District, Guangzhou 510060, Guangdong Province, China. drliuxing@163.com

Received: 2019-08-13 Accepted: 2020-04-14

Abstract

● **AIM:** To compare the damage pattern of the peripapillary retinal nerve fiber layer (pRNFL) and the macular ganglion cell-inner plexiform layer (mGCIPL) between early glaucomatous and non-glaucomatous optic neuropathy (EGON and NGON).

● **METHODS:** It is a cross-sectional study. Thirty-eight healthy controls, 74 EGONs and 70 NGONs with comparable average pRNFL loss were included. The NGON group included 23 eyes of optic neuritis (ON), 13 eyes of hereditary optic neuropathy (HON), 19 eyes of toxic optic neuropathy (TON) and 15 eyes of compressive neuropathy (CON). The sectoral pRNFL and mGCIPL thickness obtained by high definition optical coherence tomography were analyzed.

● **RESULTS:** Compared to normal controls, the pRNFL thickness in all quadrants showed a decrease in both EGON and NGON group (P<0.001), but the average pRNFL thickness of EGON group was not different to that of NGON group (P=0.94). The inferior and superior pRNFL was thinner in EGON group compared to NGON group (P<0.001). The temporal pRNFL was thinner in NGON group compared to EGON group (P<0.001). No statistically significant difference was found in nasal pRNFL between EGON and NGON. While the nasal pRNFL was thinner in CON than other three types of NGON (P=0.01), no statistically significant difference was found in other three quadrantal pRNFL among the four types of NGON (P>0.05). The mGCIPL of EGON and NGON group were thinner than control group (P<0.001). In EGON group the severest sites of mGCIPL reduction was located at inferotemporal and inferior sectors. While, compared to EGON group, the average mGCIPL of NGON group were significantly thinner, especially in superonasal and inferonasal sectors (P<0.001).

● **CONCLUSION:** The damage pattern of pRNFL and mGCIPL caused by glaucoma is distinct from other NGON such as ON, TON, HON and CON, and this characteristic damage pattern is helpful in differentiating early glaucoma from other NGON.

● **KEYWORDS:** glaucoma; optic neuropathy; retinal nerve fiber layer; ganglion cell-inner plexiform layer; optical coherence tomography

DOI:10.18240/ijo.2020.06.06

Citation: Xiao H, Liu X, Lian P, Liao LL, Zhong YM. Different damage patterns of retinal nerve fiber layer and ganglion cell-inner plexiform layer between early glaucoma and non-glaucomatous optic neuropathy. *Int J Ophthalmol* 2020;13(6):893-901

INTRODUCTION

Glaucoma is a chronic progressive optic neuropathy that causes irreversible damage to the optic nerve. Enlargement of optic disc cupping is most commonly associated with glaucomatous optic neuropathy (GON) but can also result from non-glaucomatous neurological lesions, such as optic neuritis (ON)[1], ischemic optic neuropathy[2], hereditary optic neuropathy (HON)[3], toxic optic neuropathy (TON)[4], and compressive optic neuropathy (CON)[5]. Clinically, clues such as optic nerve head (ONH) pallor can be useful in discerning non-glaucomatous from glaucomatous optic nerve cupping; however, in a study by Trobe *et al*[6] experienced observers reviewed photographs of patients with glaucoma and mixed etiologies of non-glaucomatous optic nerve cupping and often misdiagnosed the etiology of the cupping and overestimated optic nerve pallor, indicating that differentiation between glaucomatous and non-glaucomatous cupping is difficult.

High-definition domain optical coherence tomography (HD-OCT) allows accurate and quantitative measurements of peripapillary retinal never fiber layer (pRNFL) thickness and macular ganglion cell plus inner plexiform layer (mGCIPL) thickness. Studies have indicated that pRNFL and mGCIPL measurements are useful in the early detection of GON[7];

these measurements have also been used to evaluate eyes associated with neuro-ophthalmic conditions, such as multiple sclerosis, ON, non-arteritis anterior ischemic optic neuropathy (NAION) and other optic neuropathies[8-13]. Bock *et al*[11] compared the pRNFL between multiple sclerosis with or without ON and glaucoma. They found that the highest relative change of pRNFL in eyes with multiple sclerosis was in the temporal quadrant, but the highest relative change of RNFL in glaucoma eyes was in the superior quadrant. Studies[12-13] about NAION and moderate to severe stage glaucoma revealed that although the average pRNFL and total macular thickness or mGCIPL thickness were similar, the mGCIPL damage location seemed different between the two types of neuropathy. These studies indicated that both GON and non-glaucomatous optic neuropathy (NGON) could cause thinning of pRNFL and mGCIPL, but the pattern and extent of damage to pRNFL and mGCIPL seemed be different and warranted further study.

In the present study we evaluated the sectoral pRNFL, the sectoral mGCIPL and average mGCIPL thickness in early stage glaucomatous optic neuropathy (EGON) and NGON eyes with comparable average pRNFL (aRNFL) loss, as well as normal controls to further characterize and distinguish the damage patterns of optic nerve and ganglion cell between the two different types of neuropathy. As visual field (VF) test is a psychophysical examination, previous investigation[14] has reported that automated static perimetric threshold tests exhibit variability, within a test procedure and from one examination to another. Studies[15-16] have also revealed that the amount of VF variability in glaucoma and other neuropathy was much higher than normal subjects. Thus, the present study used aRNFL thickness, instead of mean deviation (MD), as a more objective and reliable matching index in the diseased groups[17].

SUBJECTS AND METHODS

Ethical Approval The study was conducted in accordance with the Declaration of Helsinki and was approved by the Institutional Review Board (IRB) of Zhongshan Ophthalmic Center of Sun Yat-sen University. Informed consent was obtained from all patients.

Patients with EGON and identified diagnosis of NGON were enrolled in this cross-sectional study. Age- and refractive error-matched healthy subjects were enrolled as controls.

The clinical diagnosis of open angle glaucoma was made by an experienced glaucoma expert (Liu X) *via* a complete ophthalmologic evaluation including best-corrected visual acuity (BCVA), slit lamp biomicroscopy examination, intraocular pressure (IOP) measurement using a Goldmann applanation tonometer, gonioscopy, axial length, stereo disc photography (Kowa nonmyd a-D III; Kowa Optimed Inc, Aichi, Japan), VF testing (Humphrey Visual Field Analyzer II; Carl Zeiss Meditec, Dublin, CA, USA), and HD-OCT scanning. Eyes that met the following criteria were diagnosed with EGON and enrolled in the study: 1) characteristic glaucomatous optic disc changes and/or repeatable glaucomatous VF defects. Glaucomatous optic disc changes were characterized as focal or diffuse neuroretinal rim thinning, localised notching, or wedge-shaped nerve fiber layer defects with correlating neuroretinal rim changes. Glaucomatous VF defects were defined by two of the following three criteria: the presence of a cluster of three points on a pattern deviation probability plot at $P<0.05$, one of which was at $P<0.01$, a pattern standard deviation at $P<0.05$, or glaucoma hemifield test results outside normal limits. 2) a VF mean deviation (MD) better than -6 dB; 3) a normal open angle; 4) exclusion of other retinal diseases such as diabetic retinopathy, age related macular degeneration, retinal vessel occlusion and so on.

Eyes with a identified diagnosis of NGON was determined by experienced neuro-ophthalmologist (Lian P), based on the etiology, symptoms, complete neuro-ophthalmic examinations including BCVA, color vision, pupil examination, slit lamp biomicroscopy examination, IOP measurement, axial length, dilated fundus examination, HD-OCT scanning, fluorescence fundus angiography (FFA), Humphrey VF test, visual evoked potential (VEP) test, cranial and orbital magnetic resonance imaging (MRI) scan, serum antibody detection and genetic screen for HON. Eyes that met the following criteria were diagnosed with NGON and enrolled in the study: 1) a history of visual loss in the eye; 2) at the time of study recruitment, at least 6mo had elapsed since the acute phase and the optic disc swelling must have subsided, and disc borders must be sharp and discrete; 3) ONH pallor was visible on slit-lamp biomicroscopy or the fundus photograph and optic nerve damage documented by a reliable VF or VEP test; 4) IOP<21 mm Hg with no history of increased IOP; 5) exclusion of glaucoma and other retinal diseases such as diabetic retinopathy, age related macular degeneration, retinal vessel occlusion and so on; 6) an aRNFL loss was matched to the mean value of aRNFL thickness in the early GON group (within ±5 μm).

Age matched normal controls were required to have at least one reliable normal result on standard automated perimetry, a normal disc appearance, no pRNFL defects, IOP<21 mm Hg with no history of increased IOP, no optic neuropathy or other ocular disease and no family history of glaucoma, optic neuropathy and other ocular disease.

The exclusion criteria for the three groups were as follows: 1) mixed or unclear diagnosis; 2) age<18 years old; 3) spherical beyond -6 to +6 diopters (D), and astigmatism >3 D; 4) poor OCT quality, defined by signal strength <6 or poor alignment on the individual OCT scans; 5) unreliable Humphrey VF testing (false positive or false negative rate >30%); 6) prior

Table 1 Demographic and baseline characteristics of patients with EGON, NGON and normal controls

Characteristics	EGON	NGON	Control	P_1	P_2	P_3	P_4
Cases (*n*)	74	70	38	-	-	-	-
Eyes (*n*)	74	70	38	-	-	-	-
Sex (female/male)	35/39	36/34	19/19	-	-	-	-
Age (y)	41.92±15.56	39.42±13.37	42.11±14.21	0.51	0.94	0.36	0.30
BCVA (logMAR)	0.06±0.10	0.22±0.29	0.00±0.08	<0.01	0.13	<0.01	<0.01
Spherical equivalent (D)	-0.79±1.80	-0.50±1.66	-0.50±1.01	0.22	0.14	0.78	0.14
Axial length (mm)	23.94±1.15	23.52±1.28	23.42±0.82	0.86	0.84	0.95	0.84
MD (dB)	-3.96±1.45	-5.95±3.55	-0.69±1.45	<0.01	<0.01	<0.01	0.10
C/D	0.73±0.11	0.64±0.15	0.43±0.14	<0.01	<0.01	<0.01	<0.01

EGON: Early glaucomatous optic neuropathy; NGON: Non-glaucomatous optic neuropathy; BCVA: Best corrected visual acuity; MD: Visual field mean deviation; C/D: Cup/disc area ratio. P_1: ANOVA was used to compare the basic information among EGON, NGON and control groups; P_2: LSD-*t* was used for EGON *vs* control groups; P_3: LSD-*t* was used for NGON *vs* control groups; P_4: LSD-*t* was used for NGON *vs* EGON groups. $P<0.05$ was considered statistically significant.

intraocular surgery or ocular trauma; 7) with neurological or systemic diseases such as diabetic, hypertension, Alzheimer's disease that could affect retina and VF results. If data from both eyes were eligible for analysis, only one randomly selected eye from each patient was included in this study.

Optical Coherence Tomography Imaging Patients with EGON and NGON were imaged by a Cirrus HD-OCT device (Cirrus HD-OCT; Carl Zeiss Meditec, Dublin, CA, USA) with 6.0 software data. Healthy volunteers recruited in the study were also imaged by Cirrus HD-OCT. Macular Cube 512×128 scan protocol centered at the foveal and optic disc cube 200×200 protocol centered at optic disc center were routinely performed for all eyes. Images with a signal strength of <6 and those with visible eye motion or blinking artifacts and segmentation failure were considered poor quality and were discarded.

The cup/disc area ratio (C/D) were generated automatically by ONH algorithm used in the Cirrus OCT software from the optic disc cube 200×200 protocol. The pRNFL software automatically extracted a peripapillary circle (3.46 mm in diameter) from the cube data set for the measurement of pRNFL thickness. The pRNFL thickness parameters (aRNFL, and superior, temporal, inferior and nasal quadrant pRNFL thicknesses) were analyzed .

The ganglion cell analysis algorithm was used to process the data obtained with the macular cube 512×128 scan protocol to calculate the thickness of the mGCIPL within a 14.13 mm^2 elliptical annular area (dimensions: a vertical inner and outer radius of 0.5 and 2.0 mm, respectively, and a horizontal inner and outer radius of 0.6 and 2.4 mm, respectively) centered at the fovea. The algorithm identifies the distance between the outer boundary of the RNFL and the inner plexiform layer as the thickness of GCIPL. The following GCIPL thickness measurements were analyzed: average and six sectoral (superior, superonasal, inferonasal, inferior, inferotemporal, and superotemporal).

Decrease Extent of pRNFL and mGCIPL We calculated the decrease extent of average and regional pRNFL and mGCIPL in EGON group and each NGON group using the following formula: decrease extent of pRNFL=($pRNFL_{EGON}$–$pRNFL_{Normal}$)/$pRNFL_{Normal}$×100% or ($pRNFL_{NGON}$–$pRNFL_{Normal}$)/$pRNFL_{Normal}$×100%. The decrease extent of mGCIPL=($mGCIPL_{EGON}$–$mGCIPL_{Normal}$)/$mGCIPL_{Normal}$×100% or ($mGCIPL_{NGON}$–$mGCIPL_{Normal}$)/$mGCIPL_{Normal}$×100%.

Statistical Analysis Statistical analyses were performed using SPSS version 16.0 (SPSS Inc., Chicago, IL, USA). Kolmogorov-Smirov test and Levene test were performed to test the normality and homogeneity of variance, respectively. Analysis of variance (ANOVA) was used to compare the basic information among EGON, NGON and normal groups as well as the parameters among different type of NGON group. Analysis of covariance (ANCOVA) model adjusted for age was used to compare the pRNFL and mGCIPL parameters among EGON, NGON and normal control groups, as well as the parameters among different types of NGON. Multiple comparisons with least significant difference test (LSD-*t*) adjustments were used for pairwise comparisons. A *P*-value of <0.05 was considered statistically significant.

RESULTS

Basic Demographics Seventy-four eyes of 74 patients with EGON, 70 eyes of 70 patients with identified diagnosis of NGON, and 38 eyes of 38 age matched healthy controls were included in this study. The basic demographics of the participants were listed in Table 1.

The NGON group included 23 eyes from 23 patients suffered from ON, 13 eyes from 13 patients suffered from HON, 19 eyes from 19 patients suffered from TON in which 3 eyes of 3 patients was diagnosed with tobacco-alcohol neuropathy and

Table 2 Demographic data of patients with NGON

Characteristics	ON	HON	TON	CON	*P*
Case (*n*)	23	13	19	15	-
Eyes (*n*)	23	13	19	15	-
Age (y)	36.48±12.48	26.69±13.05	46.42±9.92	45.33±11.94	<0.01
Sex (female/male)	14/9	2/11	6/13	11/4	-
BCVA (logMAR)	0.14±0.19	0.40±0.38	0.24±0.36	0.35±0.44	0.04
Spherical equivalent (D)	-0.65±0.87	-0.67±0.65	-0.35±0.70	-0.42±0.38	0.24
Axial length (mm)	23.75±0.98	23.84±1.00	23.24±0.82	23.58±0.94	0.85
MD (dB)	-4.15±3.22	-5.85±3.02	-5.13±2.79	-6.05±3.86	0.12
C/D	0.58±0.13	0.63±0.08	0.61±0.06	0.66±0.12	0.10

ON: Optic neuritis; HON: Hereditary optic neuropathy; TON: Toxic optic neuropathy; CON: Compressive neuropathy; BCVA: Best corrected visual acuity; MD: Mean deviation; C/D: Cup/disc area ratio. *P*: ANOVA was used to compare the basic information among different types of NGON. *P*<0.05 was considered statistically significant.

Table 3 Comparison of pRNFL thickness in EGON, NGON and normal controls mean±SD, μm

RNFL	Control	EGON	NGON	P_1	P_2	P_3	P_4
Average	100.76±5.90	86.39±5.54	86.75±8.33	<0.001	<0.001	<0.001	0.76
Temporal	79.34±14.04	68.74±10.36	47.64±10.39	<0.001	<0.001	<0.001	<0.001
Superior	124.74±15.73	106.00±12.27	115.50±15.92	<0.001	<0.001	0.002	0.002
Nasal	74.71±17.41	66.05±7.74	67.27±9.07	<0.001	<0.001	0.005	0.43
Inferior	124.55±19.58	102.79±13.13	114.61±16.05	<0.001	<0.001	0.002	0.001

EGON: Early glaucomatous optic neuropathy; NGON: Non-glaucomatous optic neuropathy; RNFL: Retinal nerve fiber layer. P_1: Analysis of covariance model adjusted for age was used to compare the RNFL parameters among EGON, NGON and normal control groups; P_2: LSD-*t* was used for EGON *vs* control groups; P_3: LSD-*t* was used for NGON *vs* control groups; P_4: LSD-*t* was used for NGON *vs* EGON groups. *P*<0.05 was considered statistically significant.

Table 4 Comparison of pRNFL thickness among different types of NGON mean±SD, μm

RNFL	ON	HON	TON	CON	*P*
Average	85.48±6.79	86.81±9.43	87.81±7.48	86.03±9.43	0.78
Temporal	45.69±8.99	47.92±10.17	48.26±10.20	49.61±13.11	0.71
Superior	116.00±9.73	115.11±18.04	118.33±15.07	113.54±22.42	0.68
Nasal	66.39±9.41	68.46±9.06	69.96±9.16	61.09±9.28	0.01
Inferior	112.74±12.91	112.42±21.38	114.21±14.24	119.91±17.70	0.54

ON: Optic neuritis; HON: Hereditary optic neuropathy; TON: Toxic optic neuropathy; CON: Compressive neuropathy; RNFL: Retinal nerve fiber layer. *P*: Analysis of covariance model adjusted for age was used to compare the RNFL among different types of NGON. *P*<0.05 was considered statistically significant.

16 eyes of 16 patients was diagnosed with ethambutol induced neuropathy, 15 eyes from 15 patients suffered from CON caused by chiasmal lesion. The basic demographics of different types of NGON were listed in Table 2.

Comparison of Peripapillary Retinal Nerve Fiber Layer Thickness The aRNFL thickness of both EGON and NGON group was thinner than that of normal controls (*P*<0.001), but the aRNFL thickness of EGON group was comparable to that of NGON group (*P*=0.94). The pRNFL thickness in all quadrants showed a decrease in both EGON and NGON group, compared to that of normal group. The pRNFL thickness in superior and inferior quadrants was significantly thinner in EGON group compared to NGON group (*P*<0.001). The pRNFL in the temporal quadrant was significantly thinner in NGON group compared to EGON group (*P*<0.001). No statistically significant differences were found in nasal pRNFL between the two groups (*P*=0.19; Table 3, Figure 1). No statistically significant differences were found in average, temporal, superior, inferior pRNFL thickness among the four types of NGON (all *P*>0.05). However, the nasal pRNFL showed statistical difference among NGON groups (*P*=0.01; Table 4), and LSD analysis revealed the nasal pRNFL of CON group was thinner than other types of NGON (all *P*<0.05).

Comparison of Macular Ganglion Cell Plus Inner Plexiform Layer Thickness The average and all six sectoral mGCIPL thickness of both EGON and NGON group was

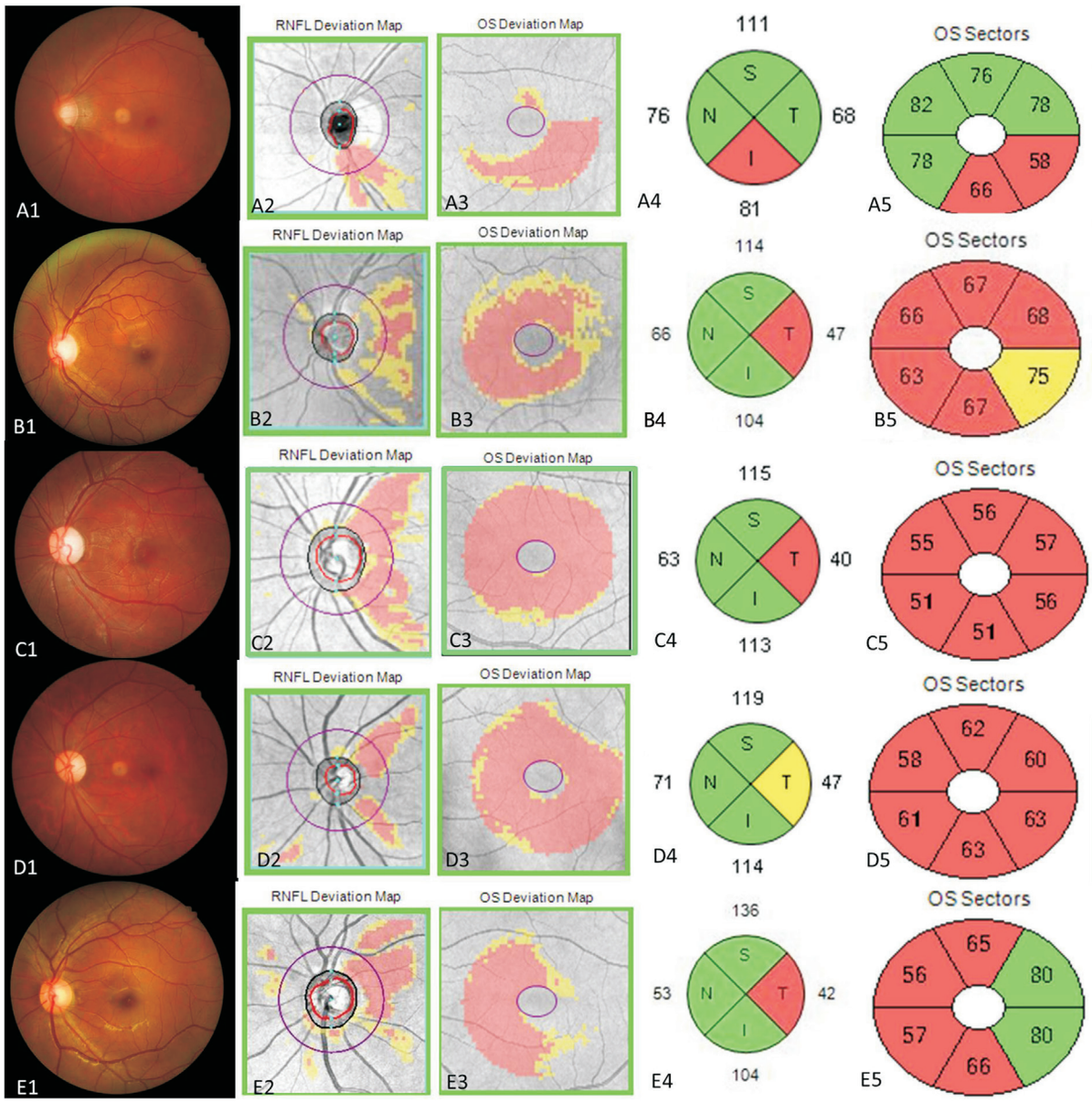

Figure 1 The pRNFL and mGCIPL of EGON and NGON A1-A5: The fundus photograph, pRNFL deviation map, mGCIPL deviation map, pRNFL thickness in the four quadrants (S: Superior; I: Inferior; N: Nasal; T: Temporal), and mGCIPL thickness in the six sectors of an EGON eye (left eye); B1-B5: The fundus photograph, pRNFL deviation map, mGCIPL deviation map, pRNFL thickness in the four quadrants, and mGCIPL thickness in the six sectors of an NGON eye induced by idiopathic ON (left eye); C1-C5: The fundus photograph, pRNFL deviation map, mGCIPL deviation map, pRNFL thickness in the four quadrants, and mGCIPL thickness in the six sectors of an HON eye (left eye); D1-D5: The fundus photograph, pRNFL deviation map, mGCIPL deviation map, pRNFL thickness in the four quadrants, and mGCIPL thickness in the six sectors of a TON eye (left eye); E1-E5: The fundus photograph, pRNFL deviation map, mGCIPL deviation map, pRNFL thickness in the four quadrants, and mGCIPL thickness in the six sectors of a CON eye (left eye). Red region indicated out of 99% distribution of normal.

thinner than that of normal controls (all $P<0.001$). The average and all six sectoral mGCIPL thickness in NGON group were significantly thinner compared to EGON group (Table 5, Figure 1). No statistically significant differences were found in average and superior, inferior, superonasal, inferonasal mGCIPL thickness among the four types of NGON (all $P>0.05$). But the superotemporal and inferotemporal mGCIPL showed statistical difference among the NGON groups (Table 6), and LSD analysis revealed the superotemporal and inferotemporal mGCIPL in CON group was much thicker compared to other three types of NGON.

Decrease Extent of pRNFL and mGCIPL in EGON and NGON Group Compared to Normal Controls Compared to normal control group, the decrease extent of pRNFL thickness in EGON group ranged from -11.59% to -17.47% among the four quadrants. The severest quadrant was inferior quadrant, followed by superior quadrant. While in the NGON group, among the ON, HON, TON and CON, the decrease extent in

Table 5 Comparison of mGCIPL thickness in EGON, NGON and normal controls mean±SD, μm

GCIPL	Control	EGON	NGON	P_1	P_2	P_3	P_4
Average	85.68±5.19	78.34±5.19	62.07±7.39	0.00	0.00	0.00	0.00
Superotemporal	84.00±5.11	78.00±6.51	63.16±8.70	0.00	0.00	0.00	0.00
Superior	86.34±5.76	81.68±5.86	62.60±8.18	0.00	0.00	0.00	0.00
Superonasal	88.24±5.74	82.65±5.86	60.60±7.85	0.00	0.00	0.00	0.00
Inferonasal	86.84±5.35	81.75±6.21	59.68±7.03	0.00	0.00	0.00	0.00
Inferior	83.46±7.26	74.85±9.85	59.41±6.88	0.00	0.00	0.00	0.00
Inferotemporal	83.92±6.11	74.20±10.16	62.43±8.51	0.00	0.00	0.00	0.00

EGON: Early glaucomatous optic neuropathy; NGON: Non-glaucomatous optic neuropathy; GCIPL: Ganglion cell plus inner plexiform layer. P_1: Analysis of covariance model adjusted for age was used to compare the RNFL parameters among EGON, NGON and normal control groups; P_2: LSD-*t* was used for EGON *vs* control groups; P_3: LSD-*t* was used for NGON *vs* control groups; P_4: LSD-*t* was used for NGON *vs* EGON groups. $P<0.05$ was considered statistically significant.

Table 6 Comparison of mGCIPL among different types of NGON mean±SD, μm

GCIPL	ON	HON	TON	CON	*P*
Average	61.52±9.09	58.63±6.01	62.33±6.04	65.60±6.00	0.11
Superotemporal	62.47±9.68	58.84±7.23	62.21±6.36	69.13±8.48	0.01
Superior	63.13±10.56	59.31±5.28	63.00±5.93	64.13±8.51	0.46
Superonasal	60.65±9.03	56.77±5.13	62.11±6.98	61.93±8.46	0.43
Inferonasal	59.04±8.73	56.08±5.04	61.26±6.23	61.80±5.58	0.32
Inferior	60.61±9.06	59.15±6.01	61.68±7.04	64.33±9.08	0.33
Inferotemporal	65.09±9.18	62.08±8.68	63.57±7.38	72.66±7.60	0.004

ON: Optic neuritis; HON: Hereditary optic neuropathy; TON: Toxic optic neuropathy; CON: Compressive neuropathy; GCIPL: Ganglion cell plus inner plexiform layer. *P*: Analysis of covariance model adjusted for age was used to compare the RNFL among different types of NGON. $P<0.05$ was considered statistically significant.

temporal pRNFL was much greater than the other quadrants (Figure 2).

Compared to normal control group, the decrease extent of mGCIPL thickness in EGON group ranged from -5.64% to -11.68% among the six sectors, and the severest sector was inferotemporal sector, and followed by inferior sector. The decrease extent of mGCIPL thickness in NGON group was much greater than EGON group. The superonasal and inferonasal sectors were the greatest mGCIPL loss region in all four types of NGON. However, in CON group, the decrease extent of superonasal and inferonasal mGCIPL thickness was much severer than that of superotemporal and inferotemporal sectors. While in ON, HON and TON group, the mGCIPL decrease extent in superonasal and inferonasal sectors was only slightly severer than that of superotemporal and inferotemporal sectors (Figure 3).

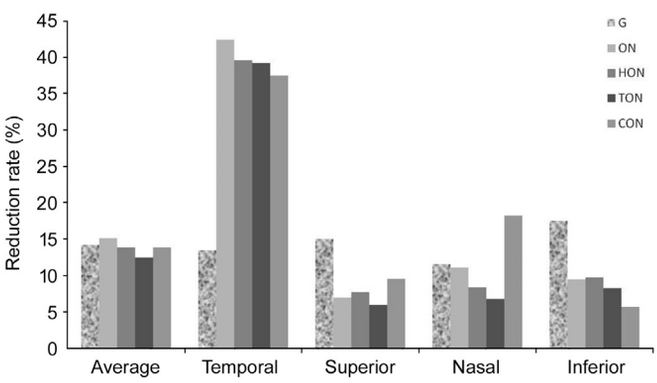

Figure 2 The mean decrease extent of pRNFL thickness in EGON and NGON groups compared to normal controls G: Glaucoma; ON: Optic neuritis; HON: Hereditary optic neuropathy; TON: Toxic optic neuropathy; CON: Compressive neuropathy.

DISCUSSION

Both EGON and NGON groups in the present study displayed enlargement of C/D area ratio compared to normal group. The same phenomenon has been documented by previous studies[1-5]. Histopathologic assessment of a patient with pathological optic disc cupping demonstrated that cupping was caused by axonal loss, with anterograde degeneration, and secondary collapse of glial support tissue resembling glaucomatous changes[18]. As both GON and NGON could cause the loss of ganglion cell and its axon, besides the enlarged cup, the loss pattern of RNFL and ganglion cell may provide more information to distinguishing GON from NGON. The loss of RNFL in glaucoma tends to be most often found in the inferior quadrant, followed by superior quadrant, has been documented in the analysis of red-free fundus photographs[19]. The similar phenomenon has also been documented by prior OCT study[20]. The present study displayed that the

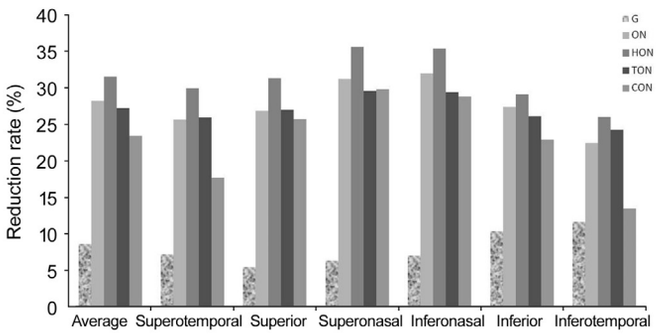

Figure 3 The mean decrease extent of mGCIPL thickness in in EGON and NGON groups compared to normal controls G: Glaucoma; ON: Optic neuritis; HON: Hereditary optic neuropathy; TON: Toxic optic neuropathy; CON: Compressive neuropathy.

inferior quadrant was the greatest pRNFL loss region in early glaucoma, followed by the superior region. The pattern of pRNFL loss may due to the pathologic change of laminar cribrosa in glaucoma. The laminar cribrosa inserts into the sclera canal wall but is not continuous with the sclera[21]. Such discontinuities between lamina cribrosa and sclera make the lamina cribrosa as the weak point of stress and strain and susceptible to damage from increased IOP and translaminar pressure gradient[21]. Based on histopathologic studies by Quigley *et al*[22], the backward bowing of the lamina cribrosa in glaucoma involved its lower and upper poles more than the mid-nerve head. The more severe deformation and remodeling in the lower and upper poles of the lamina cribrosa might result in the RNFL loss tending to be most often found in the inferior and superior quadrants in glaucoma.

The reduction of pRNFL was also found in the NGON group in this study. The whole reduction of pRNFL was comparable to that of early glaucoma group. However, the greatest loss of pRNFL in the NGON group was in the temporal quadrant. The present study included NGON induced by ON, HON, TON, and CON. Studies[23-24] about ON demonstrated that after the recovery of acute ON, the pRNFL of temporal quadrant displayed impairment in different degree. Zhang *et al*[25] also found the pRNFL was thinner in the temporal quadrant in groups of early stage of Leber's hereditary optic neuropathy (LHON). The loss of temporal pRNFL thickness was also reported in cases about tobacco and alcohol induced TON[26-27]. Danesh-Meyer *et al*'s[28] study found that the temporal and nasal pRNFL demonstrated a significantly greater proportion of thinning in CON caused by intracranial tumor. This studies also found the similar change of pRNFL in CON group. Though there were some slight difference in the change pattern of pRNFL among the four types of NGON, compared to early glaucoma group, the loss of papillomacular bundle was more common in NGON in spite of different etiologies. The different loss pattern and extent of pRNFL between EGON and NGON group may reveal the different pathological mechanism between EGON and NGON. GON is closely related to the deformation and displacement of laminar cribrosa[23]. However, the pathological mechanism of ON, HON and TON may due to Wallerian degeneration[29]. With disruption of axonal integrity, degeneration of the proximal axon segment occurs and the papillomacular bundle seems to be preferential damaged[23-27]. The preferential thinning of the temporal and nasal pRNFL with CON was recognized to be an integral part of the pattern of optic atrophy associated with classic band atrophy in patients with pure bitemporal hemianopia caused by chiasmal lesions because there is preservation of the uncrossed nerve fibers, which originate in the macular temporal hemiretina and converge to superior and inferior of ONH[28]. As the visual acuity was affected by macular retinal function, the more severe impairment of papillomacular bundle in NGON group lead to the lower BCVA in NGON group compared to EGON group. The same phenomenon was also reported in NAION with the similar pRNFL thickness compared to glaucoma group[13]. Interestingly, in spite of the comparable average pRNFL thickness, the mGCIPL was significantly thinner in the NGON group compared to GON group. The thinning of mGCIPL has been reported in ON eyes before the pRNFL edema subsided[30-31], and it was severer than the loss of pRNFL in ON eyes after the optic papilla edema subsided[10,24]. Studies documented earliest thinning region was macular area of the GCIPL map in LHON[32]. Decreased retinal ganglion cell layer thickness and volume were also detected in toxic neuropathy[33]. The present study found the same phenomenon in the ON, HON and TON groups that diffused loss of mGCIPL located in all six sectors. Moreover, the loss extent seemed severer in superonasal and inferonasal sector than in the other sectors. Tieger *et al*[34] reported thinning of the GCIPL might be detected before loss of the RNFL in some patients and binasal GCIPL loss was typical in chiasmal lesions. Blanch *et al*[35] found the GCIPL was more sensitivity to detect early chiasmal compression than RNFL and VF test. The present study revealed the thinning extent of mGCIPL were greatest in superonasal and inferonasal sector in CON group and was corresponded to the loss pattern of pRNFL. The loss pattern of mGCIPL showed some difference among CON and other NGON types. But they all demonstrated a much severer loss of mGCIPL than glaucomatous optic neuropathy and the severest location is different from that of glaucoma. In GON group, the most severe damage site of mGCIPL was inferotemporal sector, followed by inferior sector, which has been reported to be vulnerable site to glaucomatous damage[7]. The difference in the change pattern of mGCIPL provided another evidence to differentiate glaucomatous damage from other non-glaucomatous neuropathies besides pRNFL.

The present study demonstrated that the damage pattern of pRNFL and mGCIPL in early glaucoma were different from some types of non-glaucomatous neuropathies. But there were still several limitations in this study. First, this study failed to recruit NAION eyes. The pRNFL loss in most of the NAION eyes seems to be severe that reported ranged from 65.0±12.3 to 59.8±19.6 μm in previous studies[12-13], and couldn't be matched with the pRNFL loss extent of early glaucoma in this study. The different severity of pRNFL loss might affect the results. Further studies are needed to investigate the loss pattern of pRNFL and mGCIPL between GON and NGON with severer pRNFL loss and found the difference between the two at advanced stage. Second, the present research focused on the morphological difference of pRNFL and mGCIPL between GON and NGON, the combination of functional and structural changes between GON and NGON are need further investigation. Third, the loss pattern of pRNFL and mGCIPL in CON group had some differences from other three types of non-glaucomatous neuropathies, however, compared to glaucoma, the RNFL and GCIPL damage patterns of these NGON still had some common characteristic that were significantly different from glaucoma. The damage pattern of pRNFL and mGCIPL caused by GON is distinct from other NGON. And the characteristic damage pattern of pRNFL and mGCIPL in early glaucoma may provide help to facilitate comprehensive understanding of the different pathological mechanism between GON and NGON and differentiate early glaucoma from other optic neuropathies.

ACKNOWLEDGEMENTS

Foundations: Supported by the Natural Science Foundation of Guangdong Province, China (No.2017A030313649); Sun Yat-sen University Clinical Research 5010 Program (No.2014016).

Conflicts of Interest: Xiao H, None; **Liu X,** None; **Lian P,** None; **Liao LL,** None; **Zhong YM,** None.

REFERENCES

1 Rebolleda G, Noval S, Contreras I, Arnalich-Montiel F, García-Perez JL, Muñoz-Negrete FJ. Optic disc cupping after optic neuritis evaluated with optic coherence tomography. *Eye (Lond)* 2009;23(4):890-894.

2 Danesh-Meyer HV, Savino PJ, Sergott RC. The prevalence of cupping in end-stage arteritic and nonarteritic anterior ischemic optic neuropathy. *Ophthalmology* 2001;108(3):593-598.

3 Fournier AV, Damji KF, Epstein DL, Pollock SC. Disc excavation in dominant optic atrophy: differentiation from normal tension glaucoma. *Ophthalmology* 2001;108(9):1595-1602.

4 Shin YW, Uhm KB. A case of optic nerve atrophy with severe disc cupping after methanol poisoning. *Korean J Ophthalmol* 2011;25(2):146-150.

5 Blumenthal EZ, Girkin CA, Dotan S. Glaucomatous-like cupping associated with slow-growing supra-sellar itracranial lesions. *Neuro-Ophthalmology* 2006;30(5):111-115.

6 Trobe JD, Glaser JS, Cassady J, Herschler J, Anderson DR. Nonglaucomatous excavation of the optic disc. *Arch Ophthalmol* 1980;98(6):1046-1050.

7 Nouri-Mahdavi K, Nowroozizadeh S, Nassiri N, Cirineo N, Knipping S, Giaconi J, Caprioli J. Macular ganglion cell/inner plexiform layer measurements by spectral domain optical coherence tomography for detection of early glaucoma and comparison to retinal nerve fiber layer measurements. *Am J Ophthalmol* 2013;156(6):1297-1307.e2.

8 Park KA, Kim YD, In Woo K, Kee C, Han JC. Optical coherence tomography measurements in compressive optic neuropathy associated with dysthyroid orbitopathy. *Graefes Arch Clin Exp Ophthalmol* 2016;254(8):1617-1624.

9 Kupersmith MJ, Garvin MK, Wang JK, Durbin M, Kardon R. Retinal ganglion cell layer thinning within one month of presentation for optic neuritis. *Mult Scler* 2016:22(5):641-648.

10 Fukuchi M, Kishi S, Li D, Akiyama H. Acute ganglion cell loss during rapid visual recovery in optic neuritis. *Graefes Arch Clin Exp Ophthalmol* 2016;254(12):2355-2360.

11 Bock M, Brandt AU, Dörr J, Kraft H, Weinges-Evers N, Gaede G, Pfueller CF, Herges K, Radbruch H, Ohlraun S, Bellmann-Strobl J, Kuchenbecker J, Zipp F, Paul F. Patterns of retinal nerve fiber layer loss in multiple sclerosis patients with or without optic neuritis and glaucoma patients. *Clin Neurol Neurosurg* 2010;112(8):647-652.

12 Lee YH, Kim KN, Heo DW, Kang TS, Lee SB, Kim CS. Difference in patterns of retinal ganglion cell damage between primary open-angle glaucoma and non-arteritic anterior ischaemic optic neuropathy. *PLoS One* 2017;12(10):e0187093

13 Fard MA, Afzali M, Abdi P, Yasseri M, Ebrahimi KB, Moghimi S. Comparison of the pattern of macular ganglion cell-inner plexiform layer defect between ischemic optic neuropathy and open-angle glaucoma. *Invest Ophthalmol Vis Sci* 2016;57(3):1011-1016.

14 Heijl A, Lindgren G, Olsson J. Normal variability of static perimetric threshold values across the central visual field. *Arch Ophthalmol* 1987;105(11):1544-1549.

15 Heijl A, Lindgren A, Lindgren G. Test-retest variability in glaucomatous visual fields. *Am J Ophthalmol* 1989;108(2):130-135.

16 Wall M, Johnson CA, Kutzko KE, Nguyen R, Brito C, Keltner JL. Long- and short-term variability of automated perimetry results in patients with optic neuritis and healthy subjects. *Arch Ophthalmol* 1998;116(1):53-61.

17 Hood DC, Anderson S, Rouleau J, Wenick AS, Grover LK, Behrens MM, Odel JG, Lee AG, Kardon RH. Retinal nerve fiber structure versus visual field function in patients with ischemic optic neuropathy. A test of a linear model. *Ophthalmology* 2008;115(5):904-910.

18 Portney GL, Roth AM. Optic cupping caused by an intracranial aneurysm. *Am J Ophthalmol* 1977;84(1):98-103.

19 Hwang YH, Kim YY, Kim HK, Sohn YH. Agreement of retinal nerve fiber layer defect location between red-free fundus photography and cirrus HD-OCT maps. *Curr Eye Res* 2014;39(11):1099-1105.

20 Lu AT, Wang MW, Varma R, Schuman JS, Greenfield DS, Smith SD, Huang D; Advanced Imaging for Glaucoma Study Group. Combining nerve fiber layer parameters to optimize glaucoma diagnosis with optical coherence tomography. *Ophthalmology* 2008;115(8):1352-1357,1357.e1-2.

21 Crawford Downs J, Roberts MD, Sigal IA. Glaucomatous cupping of the lamina cribrosa: a review of the evidence for active progressive remodeling as a mechanism. *Exp Eye Res* 2011;93(2):133-140.

22 Quigley HA, Hohman RM, Addicks EM, Massof RW, Green WR. Morphologic changes in the lamina cribrosa correlated with neural loss in open-angle glaucoma. *Am J Ophthalmol* 1983;95(5):673-691.

23 Trip SA, Schlottmann PG, Jones SJ, Altmann DR, Garway-Heath DF, Thompson AJ, Plant GT, Miller DH. Retinal nerve fiber layer axonal loss and visual dysfunction in optic neuritis. *Ann Neurol* 2005;58(3):383-391.

24 Gabilondo I, Martínez-Lapiscina EH, Fraga-Pumar E, Ortiz-Perez S, Torres-Torres R, Andorra M, Llufriu S, Zubizarreta I, Saiz A, Sanchez-Dalmau B, Villoslada P. Dynamics of retinal injury after acute optic neuritis. *Ann Neurol* 2015;77(3):517-528.

25 Zhang Y, Huang H, Wei S, Qiu H, Gong Y, Li H, Dai Y, Jiang Z, Liu Z. Characterization of retinal nerve fiber layer thickness changes associated with Leber's hereditary optic neuropathy by optical coherence tomography. *Exp Ther Med* 2014;7(2):483-487.

26 Moura FC, Monteiro ML. Evaluation of retinal nerve fiber layer thickness measurements using optical coherence tomography in patients with tobacco-alcohol-induced toxic optic neuropathy. *Indian J Ophthalmol* 2010;58(2):143-146.

27 Ramkumar HL, Savino PJ. Toxic optic neuropathy: an unusual cause. *Indian J Ophthalmol* 2014;62(10):1036-1039.

28 Danesh-Meyer HV, Yap J, Frampton C, Savino PJ. Differentiation of compressive from glaucomatous optic neuropathy with spectral-domain optical coherence tomography. *Ophthalmology* 2014;121(8):1516-1523.

29 Gupta PK, Asrani S, Freedman SF, El-Dairi M, Bhatti MT. Differentiating glaucomatous from non-glaucomatous optic nerve cupping by optical coherence tomography. *Open Neurol J* 2011;5:1-7.

30 Behbehani R, Al-Moosa A, Sriraman D, Alroughani R. Ganglion cell analysis in acute optic neuritis. *Mult Scler Relat Disord* 2016;5:66-69.

31 Syc SB, Saidha S, Newsome SD, Ratchford JN, Levy M, Ford E, Crainiceanu CM, Durbin MK, Oakley JD, Meyer SA, Frohman EM, Calabresi PA. Optical coherence tomography segmentation reveals ganglion cell layer pathology after optic neuritis. *Brain* 2012;135(Pt 2):521-533.

32 Mizoguchi A, Hashimoto Y, Shinmei Y, Nozaki M, Ishijima K, Tagawa Y, Ishida S. Macular thickness changes in a patient with Leber's hereditary optic neuropathy. *BMC Ophthalmol* 2015;15:27.

33 Vieira LM, Silva NF, Dias dos Santos AM, dos Anjos RS, Pinto LA, Vicente AR, Borges BI, Ferreira JP, Amado DM, da Cunha JP. Retinal ganglion cell layer analysis by optical coherence tomography in toxic and nutritional optic neuropathy. *J Neuroophthalmol* 2015;35(3):242-245.

34 Tieger MG, Hedges TR 3rd, Ho J, Erlich-Malona NK, Vuong LN, Athappilly GK, Mendoza-Santiesteban CE. Ganglion cell complex loss in chiasmal compression by brain tumors. *J Neuroophthalmol* 2017;37(1):7-12.

35 Blanch RJ, Micieli JA, Oyesiku NM, Newman NJ, Biousse V. Optical coherence tomography retinal ganglion cell complex analysis for the detection of early chiasmal compression. *Pituitary* 2018;21(5):515-523.